Zr doping on lithium niobate crystals: Raman spectroscopy and chemometrics

Ninel Kokanyan, D. Chapron, Edvard Kokanyan, Marc D. Fontana

Zr doping on Lithium Niobate crystals: Raman spectroscopy and Chemometrics

Ninel Kokanyan[1,2], David Chapron,[1,2] Edvard Kokanyan[3,4] and Marc D. Fontana[1,2]

[1]*CentraleSupelec, Laboratoire Matériaux Optiques, Photonique et Systèmes, 2 rue E. Belin, 57070 Metz, France*

[2]*Université de Lorraine, Laboratoire Matériaux Optiques, Photonique et Systèmes, EA-4423, 2 rue E. Belin, 57070 Metz, France*

[3]*1Institute for Physical Research, National Academy of Sciences of Armenia, 0203, Ashtarak, Armenia*

[4]*Armenian State Pedagogical University After Kh. Abovyan, Tigran Mets Ave., 17, Yerevan, Armenia*

Raman measurements were investigated on Zr – doped lithium niobate $LiNbO_3$ crystals with different concentrations. Spectra were treated by fitting procedure and principal component analysis which both provide results consistent with each other. The concentration dependence of the frequency of the main low-frequency optical phonons gives an insight of site incorporation of Zr ions in the host lattice. The threshold concentration of about 2% is evidenced, confirming the interest of Zr doping as an alternative to Mg doping for the reduction of the optical damage in lithium niobate.

Introduction

A strong limitation to the applications of congruent commercial $LiNbO_3$ (LN) crystals in optical parametric oscillators and electro- optic devices comes from the fact that, under illumination with visible or near-infrared light, there are semi-permanent changes in the index of refraction of the crystal, due to the photorefractive (PR) effect [1]. This so-called "optical damage", causing beam distortion, dramatically diminishes the use of LN in devices. This drawback and limitation exist unless some strategy to reduce the photorefractive effect is implemented. The optical damage resistance (ODR) can be increased considerably by changing the LN crystal composition from congruent to stoichiometric [2-4] and/or by adding into LN lattice an appropriate non-photorefractive dopant [1-5]. Among the ODR dopants that have been tested, the most utilized is, nowadays, MgO that is known to be efficient in molar concentrations above 5 mol% [6]. A problem remains with this dopant owing to difficulties to grow large high optical quality MgO doped LN crystals. Recently, a set of tetravalent impurity ions (Hf^{4+}, Sn^{4+}, Zr^{4+}) as new ODR ions were checked [7-11]. It was shown that for these ions, the concentration threshold for ODR can be strongly reduced. In particular, a sample with 2mol% ZrO_2 can withstand a light intensity of 2x 10^7 W/ cm^2 of 514 nm laser. The ODR is therefore 40 times larger than that of 6.5% MgO [11]. In addition, it was shown that the non-linear optical, and electro-optical coefficients are preserved [12,13] in Zr-doped LN, so that this crystal is promising for applications of frequency conversion and laser modulation. As a consequence, Zr- doped LN with a threshold concentration of around 2-3mol% [14]. can be a good alternative to stoichiometric and/or Mg- doped crystal for reduction of the photorefractive effect. According to Kong *et al.* [11] the main question remains about the reason of the small threshold achieved with Zr doping, compared with other ODR dopant ions. In other terms the microscopic mechanism of incorporation of Zr in LN lattice is unknown and the control and improvement of this material requires the understanding of the substitution process. The threshold refers to the concentration above which the OD or PR largely decreases and is generally associated in congruent LN crystal to a complete removal of Nb antisites (i.e. the Nb ions going to the Li-site) [1]. When doping, the impurity ion can go to the site A

of native Li ions, or the site B of native Nb ions, so that in doped LN materials the PR effect can increase or decrease, according to the site occupation of the dopant.

In previous studies we have shown that Raman spectroscopy (RS) can be a useful probe of dopant ion [15, 16]. A shift of line position (optical phonon frequency) and/or linewidth (phonon damping) of some Raman lines can be thus related to incorporation of defects in the host lattice.

In the present work the Zr -doped LN crystals with different concentrations are investigated by means of Raman micro-probe, in order to have an insight of the sites occupied by Zr ions in the structure of LN and thus an understanding of the threshold concentration required for the reduction of the photorefractive effect as well.

Among all Raman lines we paid attention to those which can be used as the discriminating markers of sites A or B [17]. Thus, the lowest-frequency E[TO_1] and A_1[TO_1] Raman lines, which are associated with the motion of Nb against oxygen octahedron, can be suitably probe the site B occupied by native Nb ions. The line A_1[TO_2] corresponds to the out- of- phase vibration of Li and O and can be therefore used to study the environment of the site A and changes due to Li ions, Li vacancies and Nb antisites [17, 18].

The concentration of Zr samples in samples under study is small (below 2.5 %) i.e. much lower than the content of dopant ions used in previous works [15, 16]. Furthermore, the difference of concentrations between two "consecutive" samples in the Zr series under study is very small, so that only a subsequent very small change in Raman spectrum is expected. Chemometrics are technique able to evidence very small changes in spectra [19] and are therefore used here to support the exploitation of Raman spectra, and the dependences of vibrational modes on Zr content. Finally, the behavior of main modes vs Zr is used to derive the incorporation mechanism of Zr in the LN lattice

Experimental results and analysis

The crystals were grown by Czochralski method from congruent melts to which appropriate amounts of zirconium oxide (ZrO_2) were added. A set of samples with concentrations of ZrO_2 equal to 0.625, 1.00, 1.25, 1.50, 2.00 and 2.50 mol%, were prepared and denoted respectively as LNZr0.625, LNZr1, … Given concentrations correspond to the content of ZrO2 in the melt and are very close to those in the crystals. The relative amount of Zr in the crystals, and the presence of impurities other as Zr were checked with X-ray fluorescence. Raman measurements were carried out by means of a Horiba-Aramis spectrometer with an absolute spectral resolution of $1cm^{-1}$ and diffraction grating of 1200 $g.mm^{-1}$. The 633nm of a He-Ne laser with intensity of $1.27*10^7 W/m^2$ was used as the exciting line and the scattered radiation was detected by a CCD camera (200 pixels).

E[TO_1] and A_1[TO_1+TO_2] spectra were recorded in the $Y(XZ)\overline{Y}$ and $Y(ZZ)\overline{Y}$ backscattering configurations respectively [17, 20]. Raman spectra were carried out at room temperature and low temperature (- 180°C) as well in order to obtain more resolved lines. Indeed, lines at room or higher temperature are broader and asymmetric rendering more difficult any spectra exploitation [21].

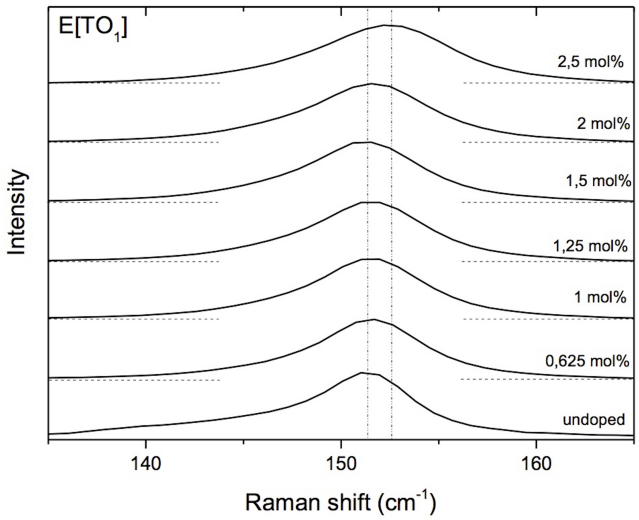

FIG 1. Raman spectra at -180°C of lowest frequency E[TO_1] mode for different concentrations of Zr in Zr- doped Lithium Niobate crystals. Vertical lines correspond to the frequency of undoped LN and LNZr2.5 samples.

E[TO_1] Raman spectra on undoped and various Zr doped LN crystals are reported in figure 1. A continuous broadening is noted with increasing Zr content while a small shift of peak maximum is observable for LNZr2 and LNZr2.5 samples as compared with all others. Spectra were fitted to damped harmonic oscillators in order to derive the frequency and the damping of phonons E[TO_1], A_1[TO_1] and A_1[TO_2]. Results are reported in figure 2.

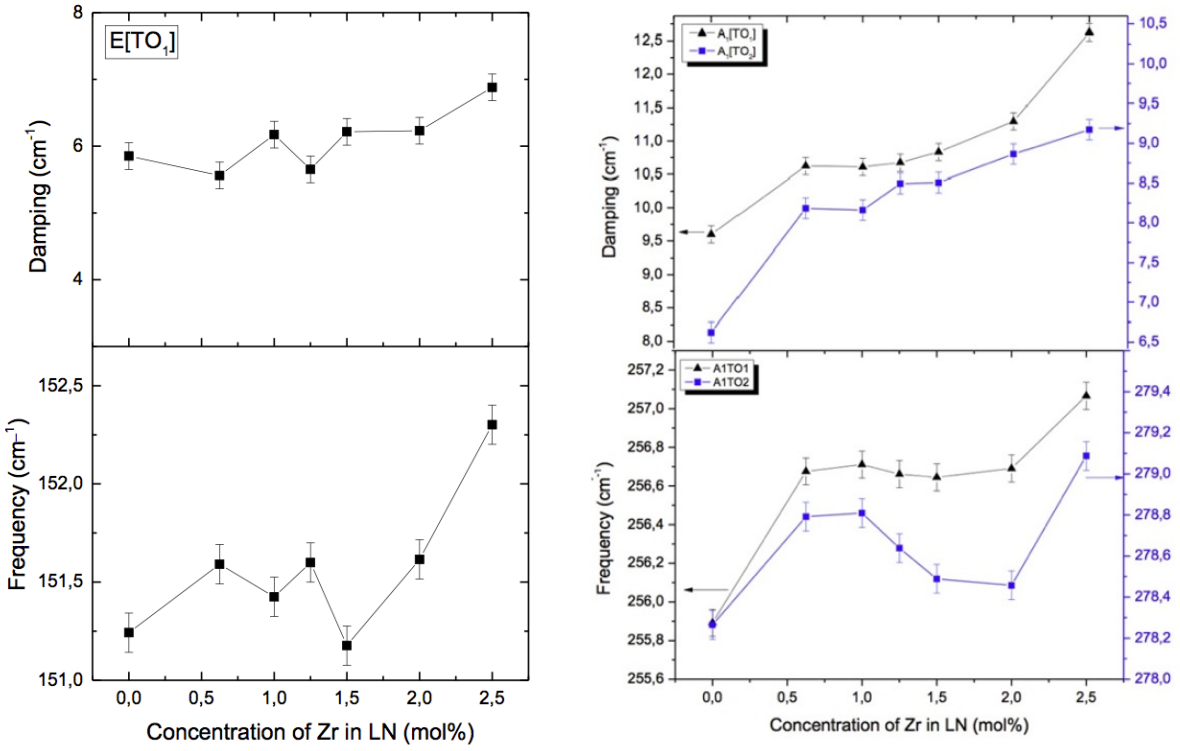

(a) (b)

FIG 2. Concentration dependence of the frequency and damping of E[TO_1] (a) A_1[TO_1] and A_1[TO_2] (b) phonons.

One can notice that the damping for each phonon under study continuously increases with doping, reflecting a growing disorder in the LN lattice, whereas the frequency exhibits a minimum value for 1.5 or 2% Zr, and then increases for larger concentrations.

This anomaly in the behavior of dependence on Zr content needed to be confirmed since only small changes of frequency were observed. Therefore, Raman spectra were additionally treated by principal component analysis (PCA), in order to evidence their relative variation with Zr concentration. Indeed, PCA is a statistical method commonly used for data classification and can be applied to the spectra analysis allowing to express their relative variability by projection on orthogonal components [22-25].

Performing a PCA on spectra we obtain the projection values of sample on each PC. The score corresponds to the relative weight of each spectrum to one component and thus gives an idea of the relative change between different samples. Loadings represent the new base, which are representative to the variation on each spectrum

$$Spectrum = \langle S \rangle + s_1 PC_1 + s_2 PC_2 + \cdots + \varepsilon \quad (1)$$

Where <S> is the average spectrum, s_i are scores, PC_i are loadings and ε are residual values. In our investigations PCA was performed using the Unscrambler10.3 software [26]. The analysis was performed after performing a standard normal variant pretreatment on the spectra utilizing the same software. The transformation is applied to each spectrum individually by subtracting the mean spectrum and scaling with the spectrum standard deviation. This means that it normalizes the intensity and corrects the baseline of all spectra.

In figure 3 are plotted different results derived from PCA applied to the spectra reported in figure 1. The components PC1 and PC2 provide 96 and 3% of the entire signal, so that they nearly reflect the whole variance. Whereas PC1 gives the change in intensity, PC2 reveals the change in the maximum peak position, since it behaves as the first derivative. The component related to line position shift (here PC2) is only used hereafter to exploit and interpret Raman data.

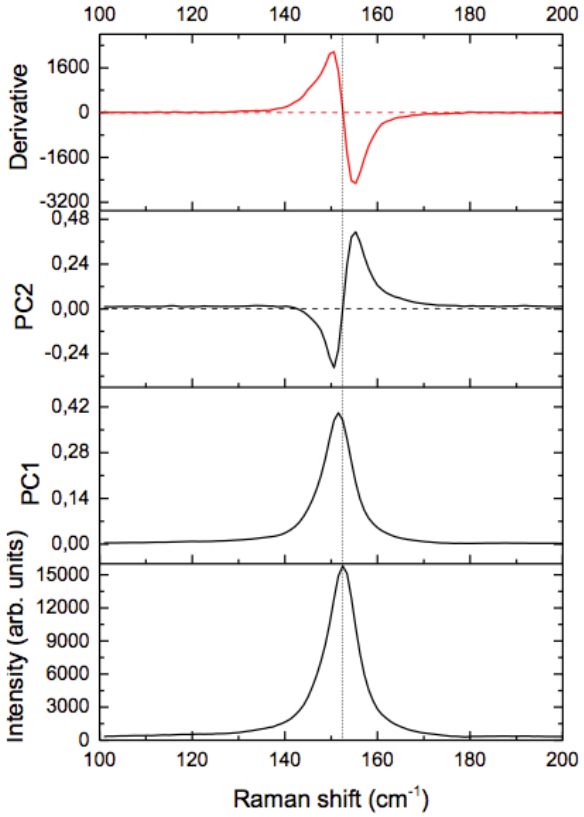

FIG 3. Loadings of PC1 and PC2 of PCA performed on the spectra (range of $100cm^{-1}$ – $200cm^{-1}$) obtained at low temperature (-180°C), for the $Y(ZX)\overline{Y}$ configuration. The spectrum of 2mol% Zr (at the bottom) and its derivative (at the top) are shown for comparison.

Scores obtained for PC2 for all spectra (or Zr contents) are plotted in fig 4 and compared with the dependence of $E[TO_1]$ frequency as derived from usual fit procedure of spectra. A similar comparison between score deduced from PC analysis and phonon frequency, for $A_1[TO_1]$ mode is reported in figure 5. In both cases the behaviors with Zr content are remarkably similar. This consistency between results derived from two completely different analysis processes from the same Raman spectra, corroborates the dependences of phonon frequency given above and renders more reliable the interpretation of these changes with Zr content.

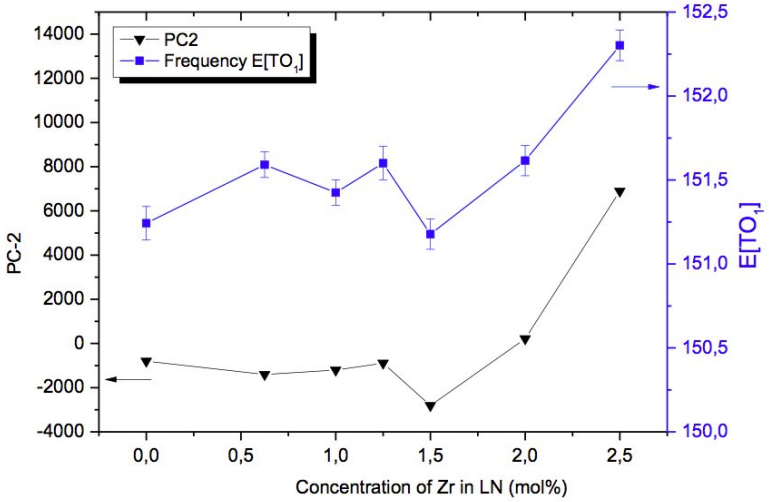

FIG 4. Frequency of $E[TO_1]$ mode and score of PC2 as a function of the Zr concentration in Lithium Niobate.

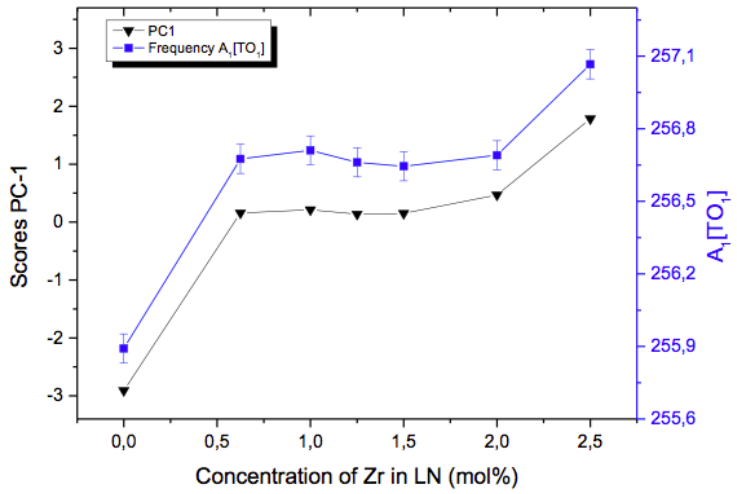

FIG 5. Frequency of $A_1[TO_1]$ mode and score of PC1 as a function of the Zr concentration in Lithium Niobate.

Interpretation and Conclusion

We are now able derive the mechanism of incorporation of Zr ions in the LN lattice from the dependences of the frequency of $E[TO_1]$, $A_1[TO_1]$ and $A_1[TO_2]$ plotted in figure 2. We remind that the modes E and $A_1[TO_1]$ mainly involve B site, while the phonon $A_1[TO_2]$ probes the site A. Furthermore, A_1 phonons correspond to ionic motions along the ferroelectric c axis, while E phonons are polarized in the plane normal to c. When they are incorporated in the LN lattice, Zr ions can at first replace Nb antisites on sites A, pushing Nb on going to their intrinsic B sites. As a consequence, the $A_1[TO_2]$ mode frequency increases due to a strengthening of A-O bond since ionic radius of Zr^{4+} is larger than Nb^{5+}, whereas the frequencies of $A_1[TO_1]$ and $E[TO_1]$ are rising as well, involving stronger B-O bond.

A more increase of the Zr concentration leads to an enhancement of the occupation of Li sites. When Zr replaces Li, as the mass of Zr ion is larger than this of Li ion, the frequency of $A_1[TO_2]$ mode decreases for concentration varying between 1 and 2mol %. In this range the frequency of phonons $A_1[TO_1]$ and $E[TO_1]$ is nearly constant. Finally, for 2.5mol% concentration the frequencies of $A_1[TO_1]$, $E[TO_1]$ and $A_1[TO_2]$ modes increase again. This can be attributed to the occupation of the Zr ions on both sites A and B as well, rendered more disordered the LN structure as reflected by the phonon damping.

It can be mentioned that Zr introduction is accompanied by a large increase of A1 phonon damping. This means that the Zr ion is slightly displaced along c axis with respect of native Li and Nb sites.

Our results show that 2% is a critical content above which the mechanism of Zr ion incorporation in LN lattice strongly changes. As shown by the behavior of phonons $A_1[TO_1]$ and $E[TO_1]$ which are both related to Nb site, the concentration 2% corresponds to the total remove of Nb antisites and therefore to the threshold of optical damage resistance. These studies confirm the interest of Zr doping for reducing the optical damage of LN.

It was shown that PCA can be useful to highlight small variations between spectra. More generally it is a fast method comparing to classical fitting method, and can be specially used in the case of a big number of samples and/or spectra in order to make a sort between samples before starting fitting procedure.

References

[1] T.R.Volk and M.Woehlecke, Lithium Niobate. Defects, Photorefraction and Ferroelectric Switching, Springer Series in Materials Science (2008).

[2] G.I. Malovichko, V.G. Grachev, E.P. Kokanyan, O.F. Schirmer, K. Betzler, B. Gather, F. Jermann, S. Klauer, U. Schlarb, M. Wöhlecke, Appl. Phys. A **56**, 103 (1993).

[3] K.Kitamura, J.K.Yamamoto, N.Iyi, S.Kirnura, J. of Crystal Growth **116**, 327 (1992).

[4] M.Fontana, K.Chah, M.Aillerie, R.Mouras, P.Bourson, Optical Materials **16**, 111 (2001).

[5] A.M.Petrosyan, R.K.Hovsepyan, E.P.Kokanyan, R.S.Feigelson, Proc. SPIE **4060**, 106 (2000).

[6] G. Zhong, J.Jin, Z.Wu, J. Opt. Soc. Am **70**, 631 (1980).

[7] E.P.Kokanyan, L.Razzari, I.Cristiani, V.Degiorgio and J.B.Gruber, Appl. Phys. Letters **84**, 1880 (2004).

[8] S.Li, S.Liu, Y.Kong, D.Deng, G.Gao, Y.Li, H.Gao, L.Zhang, Z.Hang, S.Chen J. of Physics: Condensed Matter **18**, 13 (2006).

[9] P.Minzioni, I.Cristiani, J.Yu, J.Parravicini, E.P.Kokanyan, and V.Degiorgio, Optics Express **15**, 14171 (2007).

[10] L.Wang, S.Liu, Y.Kong, S.Chen, Z.Huang, L.Wu, R.Rupp, J.Xu, Optics Letters **35**, 883 (2010).

[11] Y. Kong, Sh. Liu, Y. Zhao, H. Liu, Sh. Chen, J. Xu, Appl. Phys. Letters **91**, 081908 (2007).

[12] G. Nava, P. Minzioni, W. Yan, J. Parravicini, D. Grando, E. Musso, I. Cristiani, N. Argiolas, M. Bazzan, M. V. Ciampolillo, A. Zaltron, C. Sada, V. Degiorgio, Optical Materials Express **1**, 270 (2011).

[13] M. Abarkan, M. Aillerie, N. Kokanyan, C. Teyssandier, E. Kokanyan, Optical Materials Express **4**, 179 (2014).

[14] N. Argiolas, M. Bazzan, M. V. Ciampolillo, P. Pozzobon, C. Sada, L. Saoner, A. M. Zaltron, L. Bacci, P. Minzioni, G. Nava, J. Parravicini, W. Yan, I. Cristiani, V. Degiorgio, J. of Appl. Phys. **108**, 093508 (2010).

[15] R Mouras, M D Fontana, P Bourson, A V Postnikov, J. Phys. Condens. Matter **12**, 5053 (2000).

[16] R. Hammoum, M.D. Fontana, M. Gilliot, P. Bourson, E.P. Kokanyan, Solid State Communications **149**, 1967 (2009).

[17] M.D.Fontana, P.Bourson, Appl. Phys. Rev. **2**, 040602 (2015).

[18] V. Caciuc, A.V. Postnikov, G. Borstel, Phys. Rev. B **61**, 8806 (2000).

[19] H. Mark, J. Workman, Chemometrics in Spectroscopy, Elsevier, London, UK (2007).

[20] A.Ridah, P.Bourson, M.D.Fontana, G.Malovichko J. of Phys.: Condensed Matter **9**, 44 (1997).

[21] N. Kokanyan, D. Chapron, M. D. Fontana, Appl. Phys. A **117**, 1147 (2014).

[22] JE. Jackson, Hoboken, A User's Guide to Principal Components Analysis, NJ:John Wiley&Sons (2003).

[23] I.T.Jolliffe, Principal Component Analysis, Springer Series in Statistics (2002).

[24] T.R.Brown, R. Stoyanova, J. of Magnetic Resonance B **112**, 31 (1996).

[25] H. Witjes, M. van den Brink, W.J. Melssen, L.M.C. Buydens, Chemometrics and Intelligent Laboratory Systems **52**, 105 (2000).

[26] http://www.camo.com/rt/Products/Unscrambler/unscrambler.html